Bull. Mater. Sci., Vol. 7, Nos 3 & 4, October 1985, pp. 387–409. © Printed in India.

Neutron beam research in magnetism: The Indian scene*

N S SATYA MURTHY
Physics Group, Bhabha Atomic Research Institute, Trombay, Bombay 400 085, India

1. Introduction

I consider it a great honour bestowed on me to be able to address the Physics Section of this Session of the Science Congress.

In this address, I have chosen to give an account of the applications of neutron scattering to the study of magnetism and magnetic materials, with particular reference to our work at the Bhabha Atomic Research Centre, since this has occupied the greater part of my scientific career.

Neutron beam research being a somewhat exclusive scientific pursuit, confined to laboratories where powerful neutron sources are available, the general scientific community in India is unlikely to be aware of its growth. Therefore, I believe I will be forgiven if I take this opportunity to render á historical perspective to this narrative.

I do not do this with any claims to being a pioneer in this field. It so happened that just when I joined the Atomic Energy Establishment (now called Bhabha Atomic Research Centre) in 1958, to my good fortune, Dr P K Iyengar, the present Director of BARC, was laying the foundations of neutron spectrometry in India. APSARA, Asia's first nuclear reactor was operating and the availability of CIRUS, one of the highest flux reactors in the world at that time, was round the corner. Dr Iyengar was obviously planning a comprehensive programme of neutron beam research at CIRUS and in preparation for it, I joined him, along with Dr B A Dasannacharya, in designing and building the first neutron diffraction spectrometer. The spectrometer was built around a naval gunmount, acquired from the Naval Dockyards in Bombay and had a fair degree of automation, achieved through an a.c. motor, microswitches, uniselectors used in telephone exchanges and presettable timers. Although Dr Iyengar's interest during those days was in the study of phonon frequencies, he deliberately channelled my attention to the magnetic aspects of neutron scattering in which he had done some work himself and saw great potentialities. This spectrometer was thus first used for the study of the magnetic structure of iron-aluminium alloys. Another spectrometer, which was available a little later, was soon converted by Dr Iyengar in an ingenious way for the study of phonons by inelastic neutron scattering but, the first spectrometer came to be associated with magnetic studies. Dr Iyengar has guided me throughout my scientific career and any success our group has achieved is in great measure due to the direction and encouragement he has given us.

In all this, we were encouraged and given a free hand for determining the course of

* Manuscript originally prepared for delivering the Presidential Address of the Physics Section of the Indian Science Congress, January 1985

our work by Dr Ramanna, whose primary interests were in the study of nuclear fission using reactor neutrons. He clearly saw neutron beam research as a fertile training ground for scientists in the broader context of mastering reactor and nuclear technologies and left the details to the interests and predilections of the individual groups. Today, if the neutron scattering accomplishments at Trombay are recognised in India and abroad, it is because of the pioneering roles played by Dr Ramanna and Dr Iyengar and I dedicate this address to these two great scientists.

While my colleagues like Dr B A Dasannacharya and Dr K R Rao who joined at the same time and I were excited that we were participating in the development of a new area of experimental research, another event which greatly stimulated us around this time was the visit to our group of Prof. K S Krishnan, who was then a member of the Atomic Energy Commission. Prof. Krishnan listened to our account of the virtues of neutron scattering with such attention and reacted with such enthusiasm that we all felt we had to produce some worthwhile results by the time of the DAE Symposium at Waltair which was to be held a few months hence and which Prof. Krishnan promised to attend. The Waltair Symposium of February 1960 will always remain fresh in the memories of those who attended it. Prof. Krishnan sat through every session and had searching questions and detailed comments on how neutron scattering compared with other techniques like light scattering.

Senior colleagues like Dr Ved Prakash Duggal, Prof. N Umakantha (now at Karnatak University), Dr G Venkataraman and Dr K Usha Deniz had appreciated the magnetic applications of neutron scattering, but their interests were in the dynamical features of the magnetic interaction and they had perhaps decided that at the fluxes available in India such studies were difficult. (Nevertheless, they retained their interest in the field and, as I shall subsequently relate, the latter two led me to the study of exchange interactions in paramagnetic salts.) Much later, when we had accomplished some measure of success in magnetic structure determination by neutron diffraction, Dr L Madhav Rao and I did return to the question of measuring magnetic excitations and I shall refer to it later.

But my principal interests turned towards the use of neutron diffraction for the determination of magnetic structures and the production and application of polarised neutrons to the study of magnetic moment density distributions in magnetic materials. In this work, I have had the help and co-operation of a number of senior and junior colleagues like Dr Venkataraman, Dr Usha Deniz, Dr Dasannacharya, Dr K R Rao, Dr Madhav Rao, Dr R J Begum, Dr V C Rakhecha, Dr S K Paranjpe and Dr R Chakravarthy. In a major experimental effort of this kind, designing and building instrument plays a crucial role and in this I have had immeasurable help from Shri J N Soni, Shri C S Somanathan, Shri P R Vijayaraghavan, Shri Y D Dande and Shri M R L N Murthy. I am grateful to all of them.

My interest in the magnetic scattering of neutrons further crystallised when I spent a short period in the United States. I saw there that while several groups were already well established in the study of magnetic structures, polarised neutron spectrometers, were just being installed. I also saw briefly a polarised neutron spectrometer in operation at Brookhaven National Laboratory and several young scientists from UK and Europe trying to learn the technique. It, therefore, occurred to me that any programme that could be set up in India in the magnetic scattering of neutrons would have to include polarised neutron spectrometry to be able to compete with other laboratories. The late Dr S S Sidhu with whom I worked and Prof. C G Shull of MIT were very sympathetic to my plans for work in India. Accordingly, I resumed working with Dr Iyengar at the

CIRUS reactor (with thermal neutron flux of 6×10^{13} n/cm^2/sec) and with encouragement from him set about the task of designing and building a polarised neutron spectrometer, while organising a programme of magnetic structure studies in alloys, compounds and intermetallics. In the last two decades we have pursued investigations on magnetic materials with some success. Recently, we have been busy building new instruments for use with the more powerful DHRUVA (thermal flux 2×10^{14} n/cm^2/sec) and look forward to another useful phase of neutron beam research in India.

With these few personal remarks I shall now proceed to discuss the theory and practice of magnetic scattering of neutrons.

2. Neutron and microscopic magnetic probe

The thermal neutron possesses an intrinsic magnetic moment, a de Broglie wavelength of the order of interatomic spacings in crystals and an energy comparable with characteristic energies associated with magnetic excitations in crystals. The magnetic interaction of the neutron essentially arises from its interaction with the unpaired electrons of the atoms in the lattice while it interacts with atomic nuclei via strong interactions. It is the first interaction which is of prime interest for us here. A full and rigorous exposition of the scattering theory of thermal neutrons from condensed matter is not possible in a talk of this kind. In the next few paragraphs I shall only outline the salient features of the neutron scattering process which will help in following the later portions of this talk.

3. Principle of neutron scattering

The neutron-nuclear interaction can be taken to be a sum of δ-function potentials centred at each nucleus in the target and is given by

$$V_N(\mathbf{r}, t) = (2\pi h^2/m)\,\Sigma_i b_i \delta[\mathbf{r} - \mathbf{r}_i(t)]. \tag{1}$$

Here m is the neutron mass, b is the scattering amplitude and $r_i(t)$ is the position of the ith nucleus at time t. The neutron-nuclear interaction is short-ranged (10^{-12} to 10^{-13} cm) and for thermal neutron ($\lambda \sim 1$A) the scattering from a nucleus is isotropic.

The magnetic interaction, on the other hand, is of long range and is given by

$$V_M(r, t) = \mu_n \cdot \mathbf{M}(\mathbf{r}, t). \tag{2}$$

Here μ_n is the magnetic moment of the neutron, and $\mathbf{M}(\mathbf{r}, t)$ is the magnetisation at a position $\mathbf{r}$ at time t due to spin and orbital motions of all the unpaired electrons in the sample. Due to the spatial distribution of the magnetisation the scattering has an angular dependence or a form factor.

The most general neutron scattering experiment consists in starting with a monoenergetic, (energy E_0, wave vector $\mathbf{k}_0, |k_0| = 2\pi/\lambda_0$) polarised ($P$) neutron beam, getting it scattered from the material under study and measuring the intensity, energy (E'), wave vector ($\mathbf{k}'$) and polarisation (P') of the scattered beam. Different variants of this are followed depending upon the type of information required about the specimen. These variants may be broadly classified as diffraction (including polarised neutron diffraction) in which intensity correlation to obtain structural information is of primary interest and inelastic scattering (including quasi-elastic and polarised neutron scattering) in which energy and momentum correlation of the scattered neutrons are measured

to derive information about the dynamical features of condensed matter. Polarisation analysis of the scattered neutrons enables determination of non-collinear spin structures, isolation of magnetic diffuse scattering and separation of coherent and incoherent scattering in non-magnetic systems, such as hydrogenous material.

3.1 *Diffraction*

The nuclear scattering amplitude depends on the spin state of the scattering nucleus and is different for various isotopes of an element. Hence

$$\langle b^2 \rangle \neq \langle b \rangle^2,$$

where the symbol $\langle \ \rangle$ denotes an average over all the atoms. The scattering then consists of a coherent part whose cross-section is proportional to $\langle b \rangle^2$ and an incoherent part proportional to $\langle b^2 \rangle - \langle b \rangle^2$. The Bragg reflected intensity is related to $\langle b \rangle^2$ alone while the incoherent part gives an isotropic background modified by a temperature factor.

The cross-section for nuclear Bragg diffraction from a crystal

$$(\mathrm{d}\sigma/\mathrm{d}\Omega)_{\text{Nuclear Bragg}} = \{N_0(2\pi)^3/V_0\}\Sigma_{-\tau-}\delta(\mathbf{Q}-\tau)F_N(\tau)^2. \tag{3}$$

Here $\mathbf{Q} = \mathbf{k}_0 - \mathbf{k}'$ is the wave vector transfer of the neutron and τ is the reciprocal lattice vector. The nuclear structure factor is

$$F_N(\tau) = \Sigma_i \langle b \rangle_i \exp(j\tau \cdot r_i) \exp[-W_i(\tau)]. \tag{4}$$

The Debye-Waller factor, $\exp(-W_i(\tau))$ gives the temperature dependence of the Bragg intensities. The random variation of the neutron scattering amplitude (b) along the periodic table invests the neutron technique with certain important advantages such as the location of light elements in the presence of heavier ones and the discrimination of neighbouring elements which are difficult with x-rays. The magnetic Bragg scattering cross-section is given by

$$\begin{aligned}\mathrm{d}\sigma/\mathrm{d}\Omega_{\text{Magn. Bragg}} &= (\gamma e^2/m_e c^2)N_0(2\pi)^3/V_0 \times \\ &\times \Sigma_{-\tau-}\delta(\mathbf{Q}-\tau)F_M(\tau)^2[1-(\tau\cdot\eta)^2]_{\text{av}}.\end{aligned} \tag{5}$$

Here τ and η are unit vectors in the direction of the scattering vector and magnetisation respectively

$$\sin^2\alpha = 1-(\tau\cdot\eta)^2. \tag{6}$$

By applying an external magnetic field parallel and perpendicular to the scattering vector the magnetic scattering can be made zero or maximum respectively. The magnetic structure $F_M(\tau)$ is expressed as

$$F_M(\tau) = \Sigma \tfrac{1}{2} g_i f_i(\tau) \langle S_i \rangle \sigma_i \exp(j\tau \cdot r_i) \exp[-W_i(\tau)], \tag{7}$$

g is the gyromagnetic ratio and $f_i(\tau)$ is the form factor of the ith atom. $\langle S_i \rangle$ is the average spin at site i. The $(\pm)$ sign of the σ_i is decided by the direction of the spin at site i. The magnetic structure of the crystal can be obtained from magnetic Bragg diffraction. The magnetic form factor, f_i, on Fourier inversion gives the radial distribution of the difference between the up and down spin electrons.

$$\int f_i(\tau) 2\pi\tau \mathrm{d}\tau = \Delta p(r) = p_\uparrow(r) - p_\downarrow(r) \tag{8}$$

For polarised neutrons the corresponding cross-section is

$$(\mathrm{d}\sigma/\mathrm{d}\Omega) = N_0(2\pi)^3/V_0 x\Sigma \exp[-2W(\tau)] \langle b\rangle^2 + 2\langle b\rangle (\gamma e^2/m_e c^2) \times 1/2gf(\tau)\langle S\rangle \mathbf{P}\cdot\eta + (\gamma e^2/m_e c^2)^2\, 1/2gf(\tau)^2 \langle S\rangle^2 x\{\delta(\mathbf{Q}-\tau)\}. \quad (9)$$

Here **P** is the polarisation of the incident beam. The interference between the nuclear and magnetic scattering allows the determination of the magnitude and phase of the magnetic structure factor accurately. Fourier synthesis of the magnetic structure amplitudes provides model-independent magnetisation density distribution in the unit cell.

3.2 *Inelastic neutron scattering*

In a diffraction process, where no energy analysis of scattered neutron is involved, one essentially measures the time-averaged relative orientations of the magnetic moments or spin in the crystal lattice. The transverse fluctuations of these moments can be described as a coherent spin motion of a wavelike character of 'magnons' and the double differential scattering cross-section for neutrons is written as

$$(\mathrm{d}^2\sigma/\mathrm{d}\Omega\mathrm{d}E')_{\text{one magnon}} = (\gamma e^2/m_e c^2) \times \{1/2g\, f(Q)\}^2 k'/k_0\,(1+\cos^2\alpha)\exp\{-2W(Q)\} \times S/2x(2\pi/V_0)^3\Sigma(n_q+\tfrac{1}{2}\pm\tfrac{1}{2})\delta(h\omega_q - h\omega)\delta(Q - q\cdot\tau). \quad (10)$$

Here q is the wavevector of the magnetic excitation and $h\omega_q$ its energy. $(n_q+\frac{1}{2}\pm\frac{1}{2})$ is the population factor for magnon creation or annihilation process. It is seen that both energy and momentum conservation conditions have to be satisfied

$$\mathbf{Q} = \mathbf{k}_0 - \mathbf{k}' \quad \text{and} \quad h\omega_q = E_0 - E'. \quad (11)$$

The energies of the scattered neutrons are determined either by using a crystal analyser or by a time-of-flight measurement. Coherent inelastic neutron scattering gives magnon dispersion relations which in turn throw light on the range and strength of the magnetic interactions operative in the crystal. Since the thermal neutron possesses energy and momentum comparable to those of the magnons, the neutron scattering technique is uniquely suited to map out magnon dispersion relations in the Brillouin zone.

Having made a brief survey of the basic process and principles of neutron scattering from magnetic crystals I shall now highlight some of the important studies carried out at Trombay over the last several years in magnetic structure determination, magnetic form factor and spin density distribution studies using polarised neutrons and some inelastic studies leading to the evaluation of exchange interactions.

4. Magnetic structure studies

4.1 *Ferrites*

Ferrites constitute an important class of technologically useful ferrimagnetic materials having high permeability coupled with high electrical resistivity. Soft magnetic ferrites (those which are demagnetised at zero field) have many uses in high frequency electrical and electronic devices such as transformers, aerials, dynamos, motors, modulators,

amplifiers and as memory elements in earlier computers. Hard magnetic ferrites, on the other hand, find application in devices such as loudspeakers, recording head and magnetic tapes. Most of the soft ferrites belong to the cubic spinel structure in which the magnetic ions occupy two inequivalent lattice sites with tetrahedral (A) and octahedral (B) oxygen coordination. The magnetic structure of such crystals essentially depends upon the type of magnetic ions residing on the A and B sites and the strength of the inter- and intra-sublattice exchange interactions of the A and B sublattice J_{AA}, J_{BB} and J_{AB}. Generally J_{AB} is much larger than the other two and collinear Neel type ferrimagnetism results as in the case of Fe_3O_4. However, when J_{AA} of J_{BB} is comparable to J_{AB}, more complicated types of magnetic structures develop. A very interesting example of this type of complicated ordering was first discovered by us at Trombay, in the zinc nickel ferrites. The variation of the net ferric moment with zinc concentration is not linear and a number of previous measurements and theories had failed to explain this basic property. Zinc ferrite is completely normal (i.e. the divalent ions occupy the A sites and the trivalent ones the B sites) and becomes ordered only at very low temperatures while $NiFe_2O_4$ is completely inverted and has a high Curie point.

The neutron diffraction measurements at Trombay for a number of intermediate compositions over a wide range of temperatures established the existence of a Yafet-Kittel type of ferrimagnetic arrangement in these ferrites as shown in figure 1. These ferrites, have, in fact been shown by the Trombay results to possess two regions of magnetic ordering: one, a canted Yafet-Kittel type and the other, a collinear, Neel type of ordering with two-well-defined transition temperatures.

This is illustrated in figure 2. These complicated spin arrangements are due to the competition of as many as five exchange interactions and explain many of the ferrimagnetic resonance parameters of these ferrites. Beautiful confirmation of these

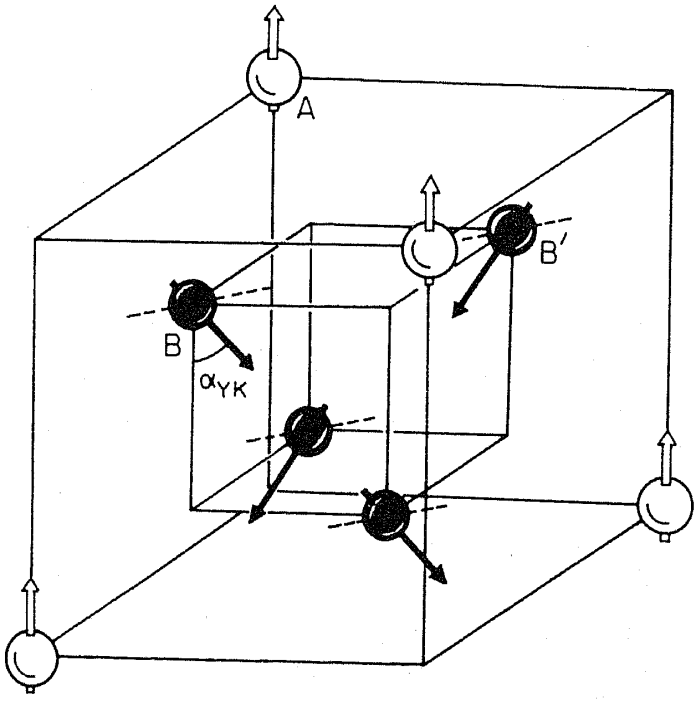

Figure 1. Three-dimensional representation of Yafet-Kittel structure in a spinel ferrite.

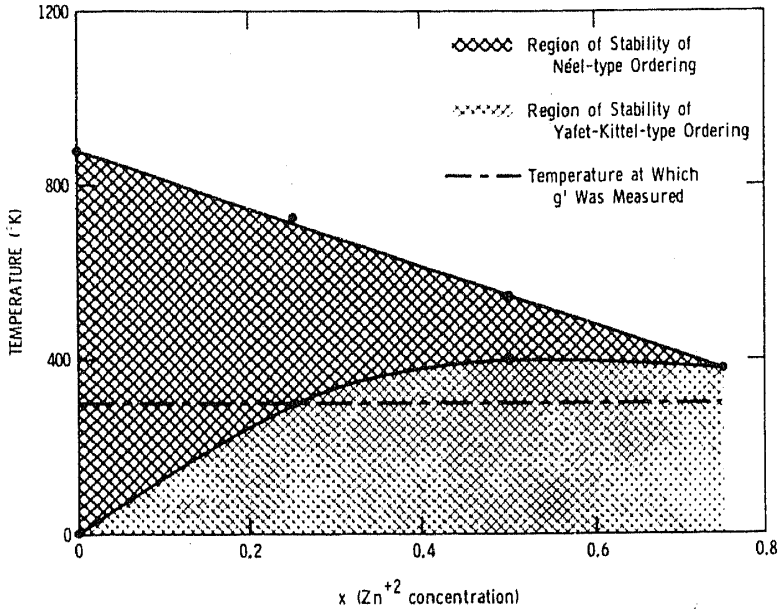

Figure 2. Magnetic order in $Zn_xNi_{1-x}Fe_2O_4$ system as determined from neutron diffraction measurements.

results has been obtained by Scott and Reck in their Einstein-de Haas measurements of the magnetomechanical ratios of these ferrites which are also shown in figure 2.

Another class of mixed ferrites in which a similar non-collinear moment arrangement was discovered by neutron diffraction by us was the Co-Zn ferrite system. Figure 3 summarises the variation of the Yafet-Kittel angles with temperature in these ferrites.

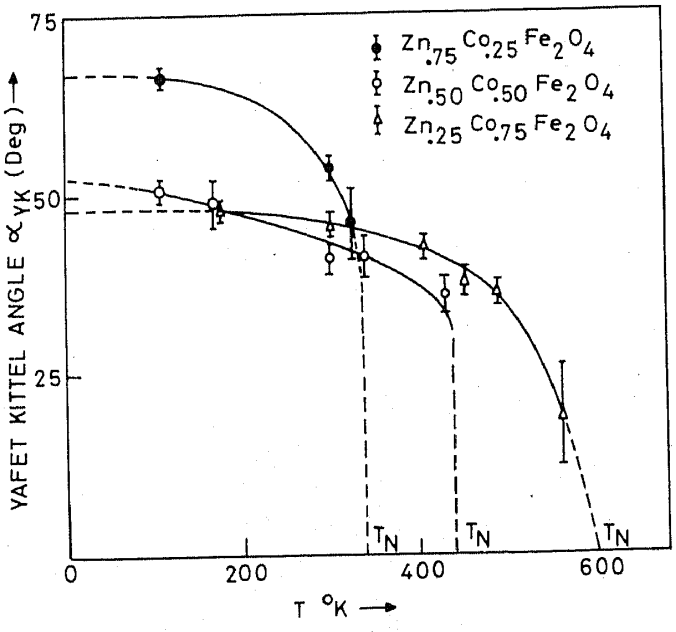

Figure 3. Variation of the Yafet-Kittel angle with temperature in $Co_xZn_{1-x}Fe_2O_4$ for $x = 0{\cdot}25$, $0{\cdot}50$ and $0{\cdot}75$.

An interesting feature here is the absence of a Neel region as in Ni-Zn ferrites. The existence of Yafet-Kittel type spin ordering was subsequently confirmed by Mössbauer measurements by several workers on these materials. These experiments have thus superseded earlier theoretical notions according to which cubic normal spinels could not support a Yafet-Kittel spin canting. Similarly, a powder diffraction study on another spinel, Co_2TiO_4 (in which both the Co ions are on the *B* site) at 4 K revealed that this substance has a spiral magnetic ordering. I would like to recall here the careful data gathering and analysis made by my early students, Dr M G Natera from the Philippine Atomic Research Centre and Dr S I Youssef from the Atomic Energy Centre of Egypt who participated in these investigations on the ferrites.

Quite often, the solution of the magnetic structures of the mixed ferrites of the type discussed above presents difficulties because of insufficient data and the number of parameters to be determined (cation distribution, magnetic moments and moment orientation etc). This problem is particularly acute when single crystal specimens are not easy to prepare. The use of polarised neutron powder diffraction in such instances was emphasised by us and successfully used in a number of instances. This was exploited by us in the elucidation of the structure of manganese cobalt carbide and the spinel ferrites. I shall refer to this technique in connection with our recent work on Mn_4N. The potentiality of this technique is indeed great and has not been fully exploited.

4.2 *Heusler alloys*

Heusler alloys with the chemical formula X_2MnY exhibit chemical order characteristic of compounds and at the same time have high metallic conductivity. Their magnetic properties are also intermediate between those of ionic compounds and of transition metals. The crystallographic structure of this class of alloys can be conceived as eventually arising due to the interpenetration of 4 fcc sublattices belonging to the X, Mn and Y atom species. The chemical (atomic) and magnetic structure of the Heusler alloys with X = Pd, Cu, Co and Y = Ge, Sn, In and Sb were studied at Trombay several years ago to arrive at an understanding of the ferro- or antiferromagnetic structure of these alloys in terms of magnetic ion separation, and partial disorder. Much later, the series $Cu_{2-x}Pd_xMnAl$ was studied as a function of x to understand the role of the X atom on the magnetic structure of the alloy (Cu_2MnAl is ferro-magnetic while Pd_2MnAl is antiferromagnetic). It was found that the transition from the ferro-magnetic to the antiferromagnetic state occurs somewhere in between $x = 0{\cdot}8$ and $0{\cdot}9$. The magnetic ordering temperature was found to initially decrease with x, reaching a minimum and then increasing again.

5. Magnetic form factor and spin density distributions using polarised neutrons

Polarised neutron diffraction has been an extremely valuable technique for studying outer electron distributions in magnetic material through measurements of magnetic form factors. The principal motivation in undertaking the measurement of magnetic form factors with polarised neutrons has always been to gain a better understanding of solid state electronic wave functions. How are the outer electron densities of free atoms changed when the atoms are brought together in condensed matter? Equations (7) and

(9) of § 3 can be rearranged to show that there can be interference between nuclear and magnetic scattering if there is no change of spin direction in the Bragg scattering process. That is, for the non spin-flip process $\uparrow\uparrow$, the Bragg cross-section is

$$(d\sigma/d\Omega)_{\uparrow\uparrow} \sim |F_N(\tau) + \mathbf{P}\cdot F_M(\tau)|^2. \tag{12}$$

Figure 4 shows the schematic of an instrument for polarised neutron diffractometry. A monochromatic polarised neutron beam is produced by Bragg reflection of polychromatic unpolarised neutrons from the reactor by a polarizing crystal. The ideal polarising crystal (the (200) plane of $Co_{92}Fe_{08}$ crystal is an example) has $F_N(\tau) = F_M(\tau)$ so that by equation (12) it has zero cross-section for neutrons polarised antiparallel to $F_M(\tau)$ and a large cross-section for the reverse polarisation.

The polarisation is maintained in the flight path to the specimen by magnetic guides producing fields in the polarising direction. At a suitable point in this path a 'spin flipper' is introduced. This may be a radiofrequency (RF) coil tuned to the Larmor frequency as in the original diffractometer described by Nathans *et al* and in Trombay, or one of a number of other devices. The purpose of the spin flipper is to reverse the neutron polarisation when it is 'on' and allow the neutrons to pass unchanged when it is 'off'. In a polarised neutron experiment, the diffractometer and sample are set so that the peaks of a Bragg reflection enter the detector and the ratio between the counting rates for the two polarisation states is measured. This ratio, commonly known as the 'polarising ratio' or 'flipping ratio' is recorded for each reflection and these ratios (R) constitute the basic raw data of the experiment. Figure 5 brings out the disposition of the various magnetic fields in the Trombay polarised neutron spectrometer. Table 1 lists the parameters of the Trombay polarised neutron spectrometer.

In centrosymmetric structures when both $F_N(\tau)$ and $F_M(\tau)$ are real and the neutron polarisation is parallel to the magnetisation and perpendicular to the scattering vector, the ratio R is

$$R = \{F_N(\tau)^2 + F_M(\tau)^2 + 2F_M(\tau)F_N(\tau)\}/\{F_N(\tau)^2 + F_M(\tau)^2 - 2F_M(\tau)F_N(\tau)\} = (1+\gamma/1-\gamma)^2 \tag{13}$$

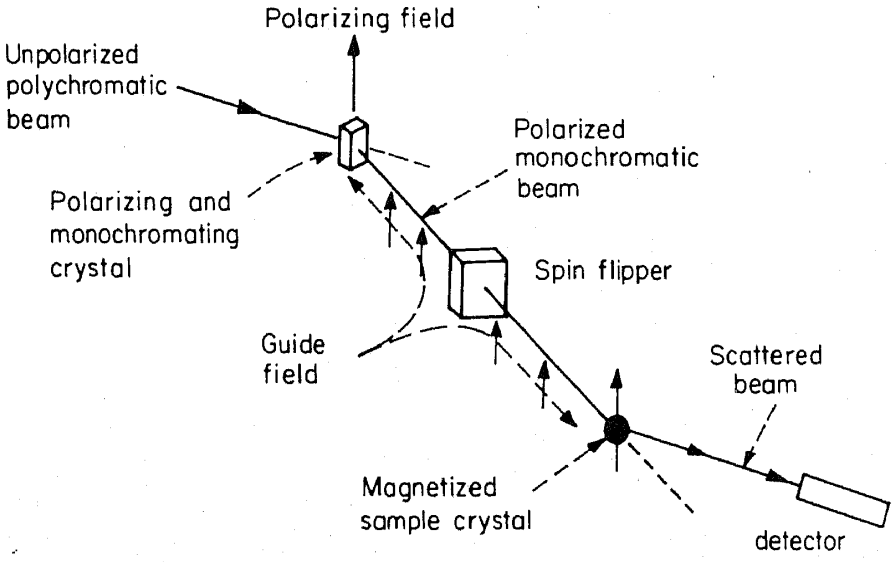

Figure 4. Schematic representation of a polarised neutron diffraction spectrometer.

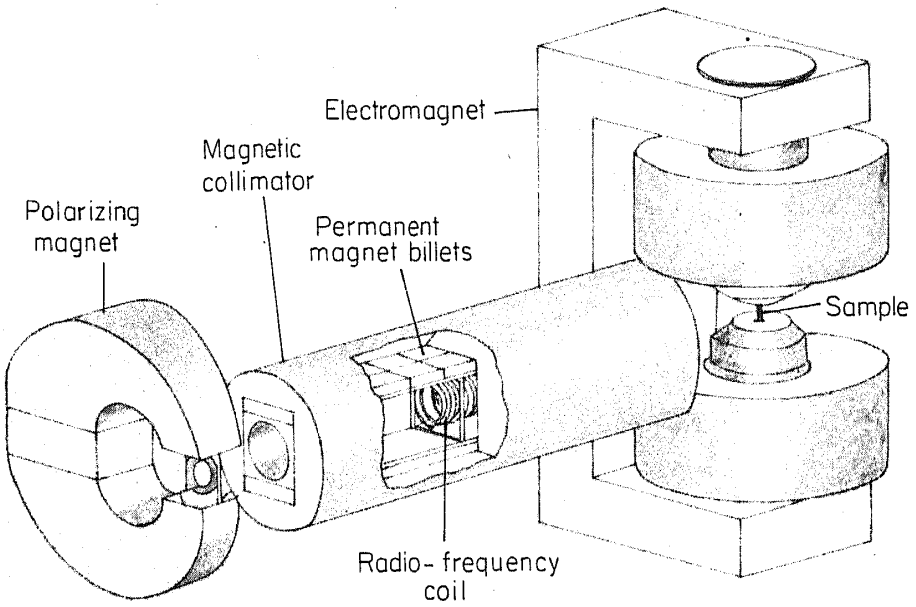

Figure 5. A perspective view of the magnets in the polarised neutron spectrometer at Trombay. The cut-away section reveals the radio-frequency coil used for reversing the neutron polarisation.

Table 1. Parameters of the Trombay polarised neutron diffractometer

Neutron wavelength	0·92 A
Polarised neutron flux at sample position	2×10^4/cm^2/sec
Second order contamination	< 1%
Polarisation efficiency	97%
Flipping efficiency	100%
Polarising field	0·3 Tesla
Guide field	0·012 Tesla
Flipping frequency	343 kHz
Analysing field	0 to 2 Tesla

where $\gamma = F_M(\tau)/F_N(\tau)$. The point I wish to emphasise here is that the polarised neutron technique fixes the relative phases of the magnetic and nuclear scattering experimentally in centrosymmetric structures. Obviously a precise evaluation of the magnetic structure factors presupposes a knowledge of precise $F_N(\tau)$'s.

Equation (13) assumes perfect polarisation and perfect spin reversal efficiency of the RF coil and the absence of systematic errors principally due to extinction. While it is rather simple to correct for the first two, considerable caution has to be exercised in accounting for the presence of extinction in order to obtain accurate values of $F_M(\tau)$ from the measured polarisation ratios.

With the knowledge of the phase and magnitude of the magnetic structure factors over a wide region in reciprocal space, one can Fourier-synthesise them, using standard averaging procedures to obtain model-independent magnetic moment density distributions in any crystal plane. Alternately one can interpret these measured magnetic

structure factors in Fourier space (reciprocal space) itself to obtain information about the asphericity of the local moment, the magnitude of the local moment, diffuse moment, etc. The different theoretical approaches to the interpretation of polarised neutron data have been discussed elsewhere. Here I confine myself to bringing out the essential physics that has emerged in different systems studied at Trombay.

5.1 *An intermetallic system, MnAlGe*

MnAlGe is an intermetallic compound, isomorphous with Mn_2Sb (both have the tetragonal structure) in which one of the Mn atoms is replaced with Al and Sb replaced by Ge. The site symmetry of the Mn atom is tetrahedral with a tetragonal field surrounded by the Al and Ge atoms. The observed magnetic structure factors were fully analysed in Fourier space to obtain the fractional occupancy of the magnetic moment in the various symmetry orbitals appropriate to the tetragonal field. The significant outcome of this analysis was the highly non-spherical distribution of magnetic moment density around the Mn atom with a large fractional occupancy of the A_{1g} orbital disposed along the tetragonal axis, which happens to be the easy direction of magnetisation. Figure 6 attempts to convey a pictorial impression of the asphericity of this moment density.

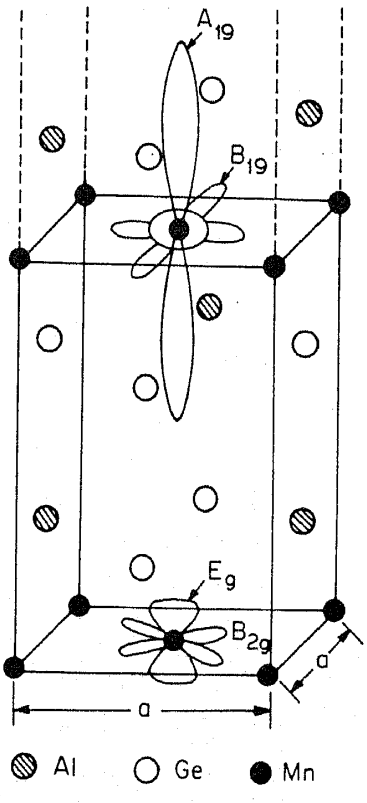

Figure 6. Pictorial representation of the four-symmetry orbitals of the Mn atom in MnAlGe. For clarity, all the four orbitals have not been shown on the same atom.

5.2 *Ionic system*

Magnetic scattering from ionic crystals has been generally discussed in terms of molecular orbitals of transition metal complexes. This is useful both for relating trends between one ligand and another and also for comparing neutron data with those got from resonance studies of ligand hyperfine interaction (LHFI). Deviations from a simple ionic model introduced by covalency effects are generally quite small ($\sim 10\%$) making it important for a proper interpretation of the neutron data to know the metal ion ground state wavefunction. Consequently, a majority of covalency studies have been confined to systems with spin-only ground states, but even here the interpretation of the experimental observation is by no means trivial. Hubbard and Marshall for the first time discussed the determination of covalency parameters from neutron scattering experiments almost a decade after LHFI was first observed by Owens and Stevens. The time lag between these two developments reflects the difficulties underlying the determination of the magnetic form factors of the desired precision, which situation has now considerably improved, thanks to the availability of better neutron fluxes and better neutron beam research techniques. Figure 7 shows how the presence of ligand and overlap densities modify the 'free ion' magnetic form factor.

5.2a Fe_3O_4: As an example of the molecular orbital approach (Hubbard and Marshall) to interpret covalency effects from polarised neutron data, I shall discuss briefly the interpretation of the experiment on Fe_3O_4 done at Trombay a few years ago. Fe_3O_4 is an inverted cubic spinel ferrite in which the tetrahedral (A) sites are occupied by Fe^{3+} ions and the octahedral (B) sites are randomly occupied at room temperature, by equal numbers of Fe^{2+} and Fe^{3+} ions. Using the form factor approach, attention was specifically focussed on the moment distribution of the Fe^{3+} ion on the *A* site (this

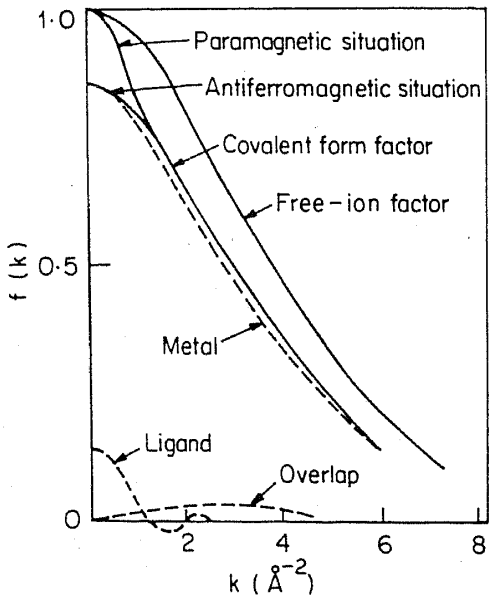

Figure 7. Typical form factors for a 3*d* ion based on a simple molecular-orbital theory. The free ion form factor and the covalent form factor for both the paramagnetic and antiferromagnetic situations are shown. The dash lines indicate the three components of the covalent form factor due to the metal ion spin, the ligand spin and the overlap spin.

study yielded a more accurate value of the magnetic structure factors than an earlier one conducted by us, principally on account of the use of thinner crystals which reduce considerably systematic errors arising out of extinction).

The tetrahedral crystal field splits the d level into two groups but with the E set lower than T_2. We recall that in a pure crystal field situation, even in the absence of symmetry the moment density at A will remain centrosymmetric (see figure 8) and its form factor will be real. However, when one allows for covalency this is no longer true.

The magnetic form factor will have an imaginary component $f_3(k)$ i.e.

$$f(\mathbf{k}) = f_0(\mathbf{k}) - iB(hkl)f_3(\mathbf{k}) + A(hkl)f_4(\mathbf{k}). \tag{14}$$

We calculate the overlap form factors corresponding to a given overlap density using Slater-type orbitals for Fe^{3+} given by Clementi and those of O_2 given by Watson. The admixture coefficients which remain as adjustable parameters then determine to what extent the overlap form factors for the various crystal field states contribute to the net form factor for the A site density. The covalency parameters for the A site ($A_\sigma^{T_2}$, $A_\pi^{T_2}$ and A_π^{E}) were sought by direct comparison of the calculated magnetic structure factors

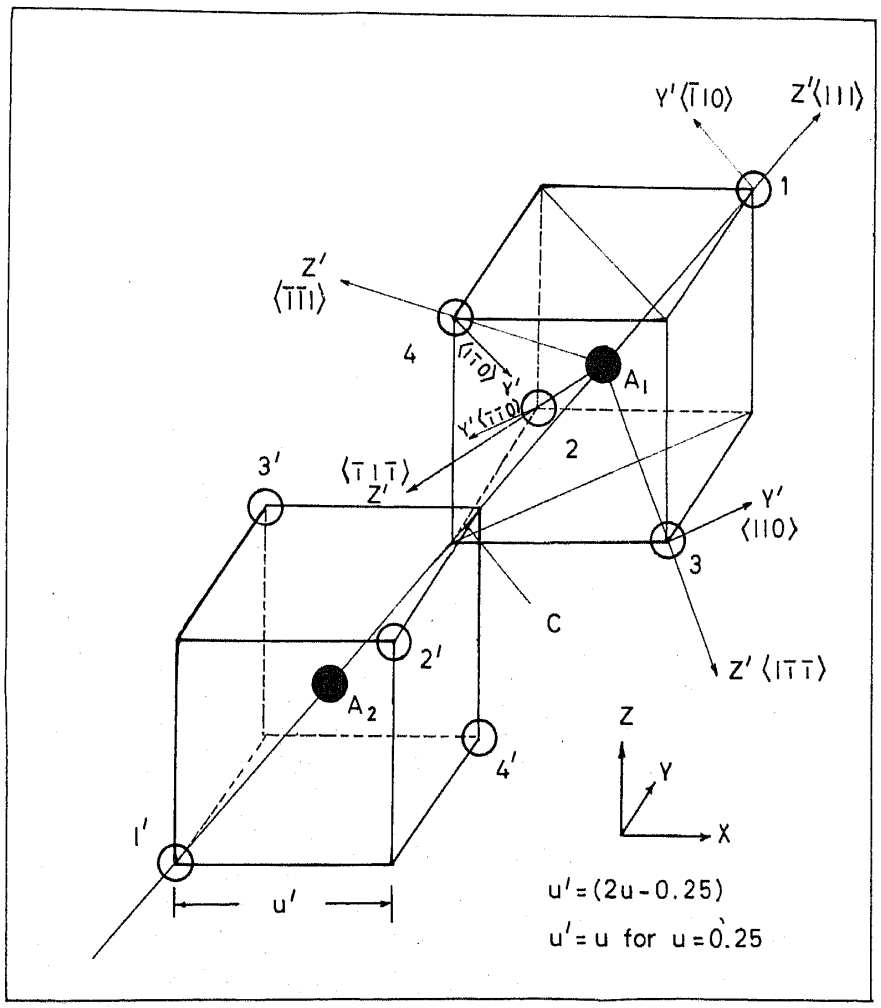

Figure 8. Two neighbouring A sites in the unit cell, denoted by A_1 and A_2 together with their nearest neighbour oxygen tetrahedra.

with the experimental ones by a least-squares procedure (see figure 9). This study leads to the conclusion that about 28% of the moment density is transferred from the *A* site to the neighbouring oxygen ligands (i.e. about 7% each). Quantitative evaluation of covalency parameters (using an ab initio theoretical approach) of the Fe^{3+} ion in a tetrahedral environment from an experimental study was the first of its kind.

5.3 *Disordered ferromagnetic binary alloys*

The 3*d* ferromagnets were the first class of materials to be studied with the polarised beam technique in the 60's at MIT, USA by Prof. Shull and his students. From the analysis of magnetic structure factors and from the moment density maps, definite departures from spherical symmetry were observed for iron, nickel and fcc cobalt while hexagonal cobalt showed nearly spherical symmetric moment distribution (in cubic crystals, the degree of symmetry of the moment distribution is denoted by *p*, the fractional population of the moment in the E_g orbitals. For a spherically symmetric distribution $p = 0{\cdot}4$). It was found that iron has a decidedly large E_g symmetry with $p = 0{\cdot}54$ while nickel has a pronounced T_{2g} symmetry with $p = 0{\cdot}19$. Another important feature in all these maps is the existence of a uniform negative diffuse moment density in the interstitial region. Figure 10 shows a moment density map in

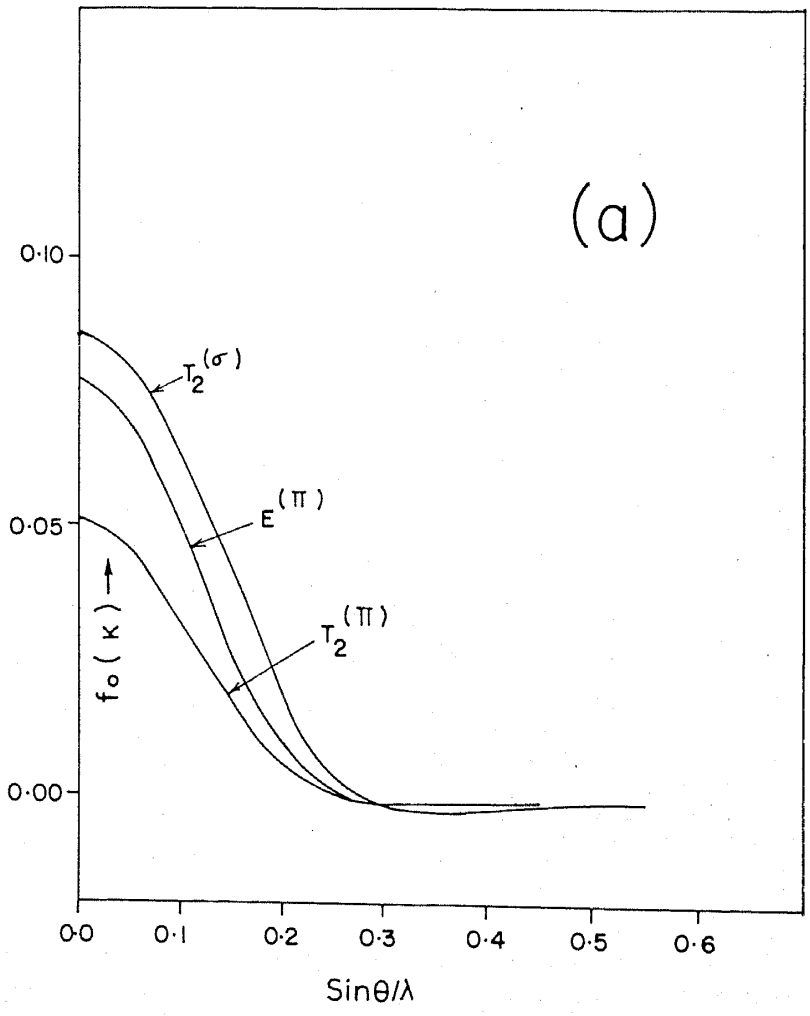

Figure 9. For caption, see p. 402.

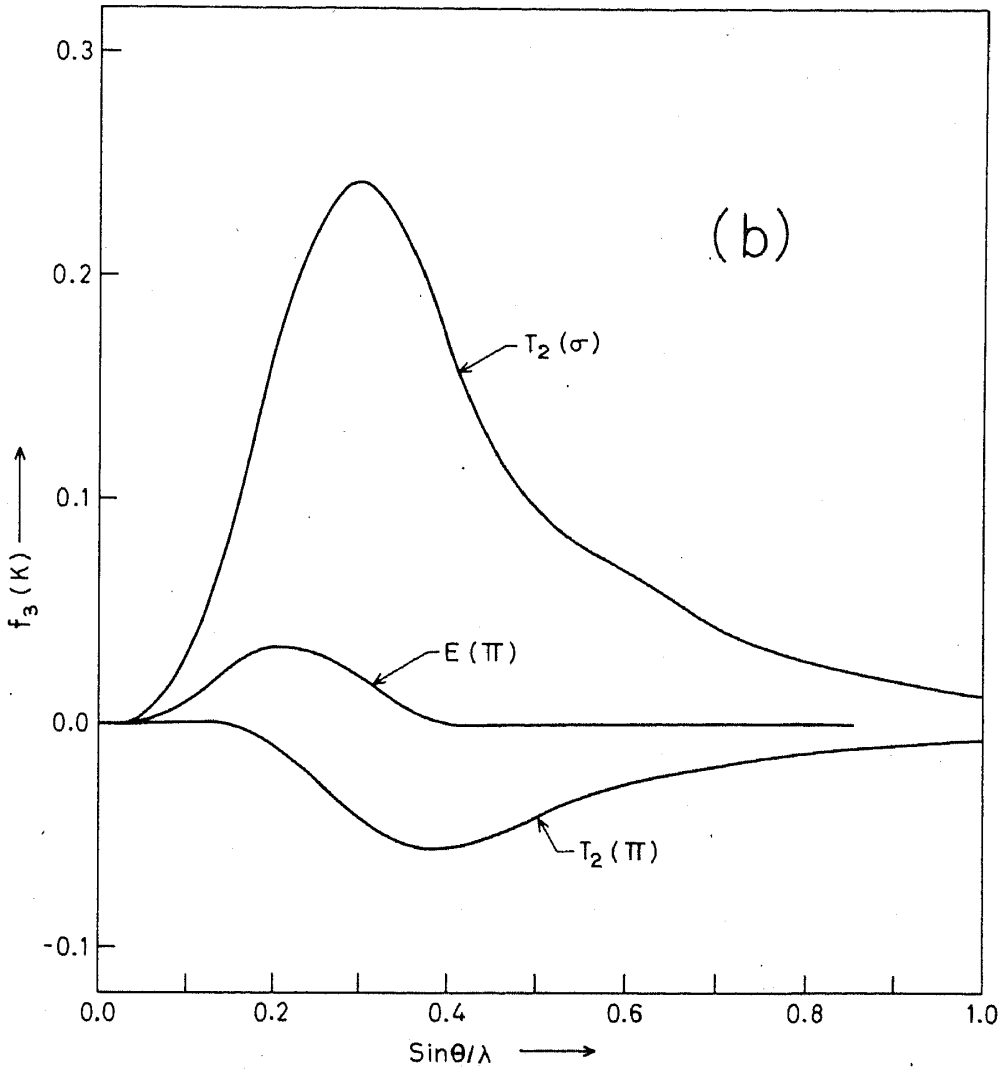

Figure 9. For caption, see p. 402.

nickel where these features are clearly seen. Very much later, the polarised beam technique was used in a variety of ferromagnetic **3d** – 3*d* alloys to study the detailed concentration dependence of (a) the magnetic moment distribution (b) the asphericity of the local moment and (c) diffuse moment density. Such experimental studies provide a useful testing ground to check band theoretical predictions, especially in regard to (a) and (b). The first systematic polarised neutron study of moment density distributions in a 3*d* alloy with 4*d* impurities was undertaken by us. The system we investigated was a series of ferromagnetic $Ni_{1-c}Ru_c$ alloys. This particular 3*d* – 4*d* dilute system was chosen for our study because transport property measurements in the NiRu alloys gave indirect evidence of the formation of an impurity virtual bound state very near the Fermi level. In this picture, one should expect to find fairly extensive magnetic perturbations in the lattice. Magnetic structure amplitudes obtained from the polarised neutron data were analysed using the form factor approach as also in terms of moment density maps. A significant feature of these maps is the fairly strong perturbation

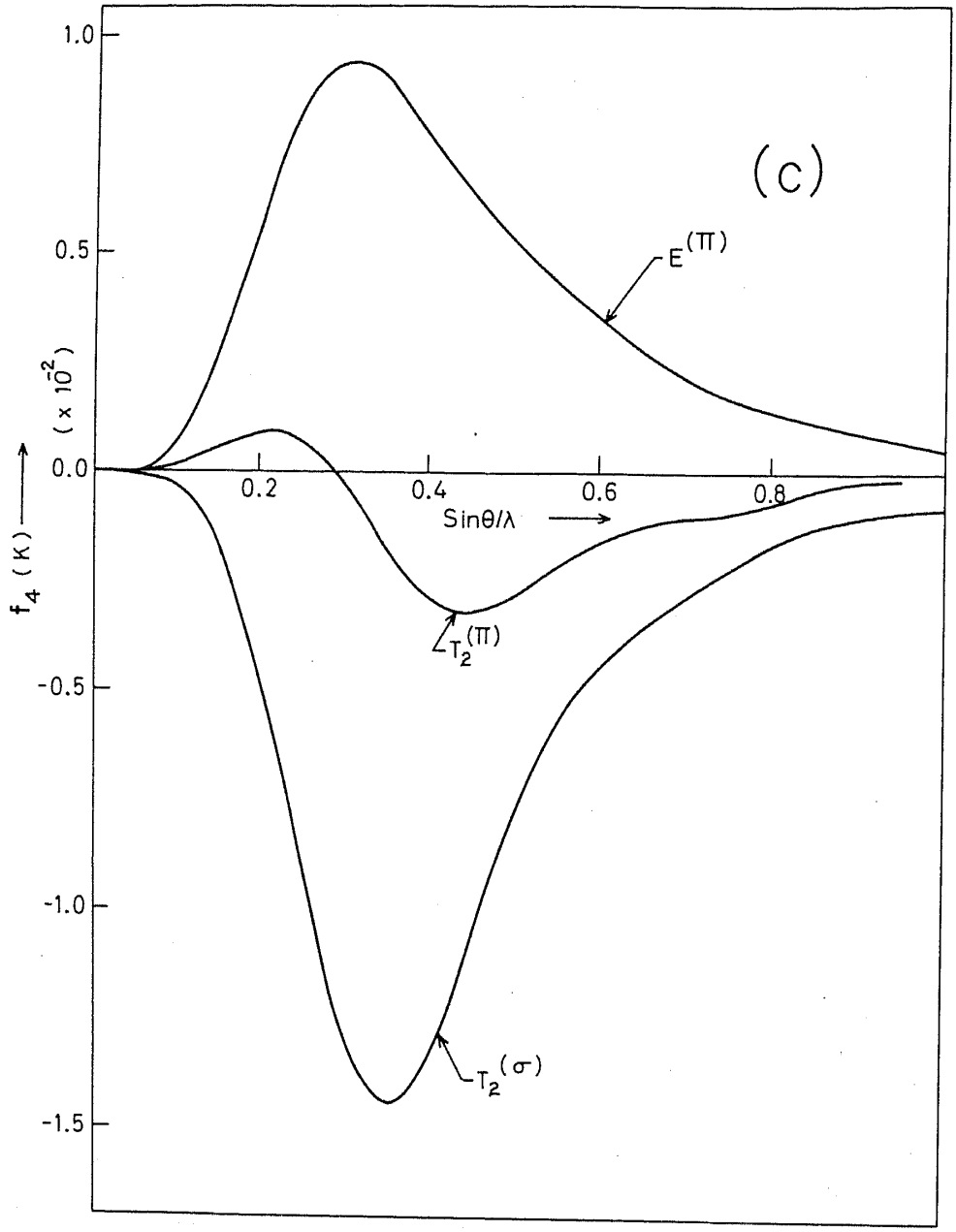

Figure 9. The form factors for overlap densities $\langle d_T/\psi_{T\sigma}\rangle$, $\langle d_T/\psi_{\pi}\rangle$ and $\langle d_E/\psi_{E\pi}\rangle$. (**a**) f_0 (**b**) f_3 (**c**) f_4.

introduced by the Ru impurity on the diffuse moment density i.e. at positions of the unit cell far removed from the atomic sites. Whereas in nickel, Moon had observed a uniform negative diffuse moment density in these regions we observed in NiRu "islands" of positive and negative diffuse density which grew at the expense of each other with increasing Ru concentration. Figure 10 illustrates this feature. The magnetic asphericity parameter, however, was not significantly different from that in pure Ni except at the highest concentration ($c = 0{\cdot}046$) studied. Another interesting feature observed by us in the NiRu alloy system was that the alloy form factor was sharper than in pure Ni, the average sharpness varying from 0·7% to 3·5% over the impurity

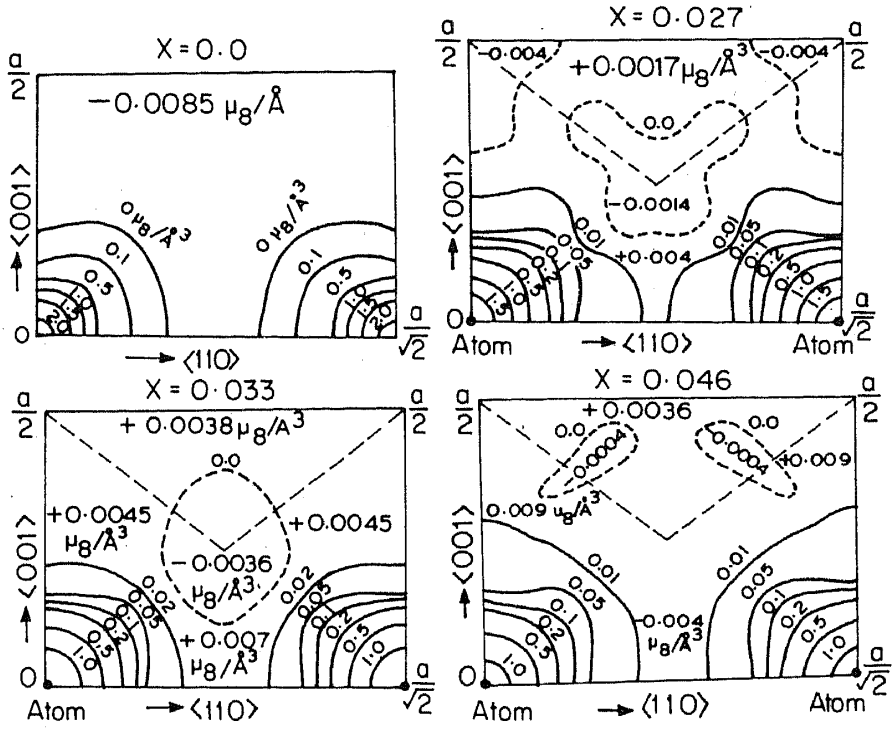

Figure 10. Moment density map in the (110) plane in nickel ($x = 0$) and in $Ni_{1-x}Ru_x$ ($x = 0{\cdot}027$, 0·033 and 0·046). Note the uniform negative diffuse moment density in the interstitial region seen in pure Ni gets transformed into varying positive and negative islands of diffuse moment density for different Ru impurity concentration.

concentration range. The coherent potential approximation (CPA) is generally considered as the most advanced approximation to describe the electronic structure of random alloys. A multiband CPA calculation carried out in this laboratory on the Ni-Ru system was able to explain broadly the experimental features and also predict the formation of Ru virtual bound states near the Fermi level (see figure 11).

Another binary random ferromagnetic alloy system studied by us was Ni_{1-c} Cr_c ($c = 0{\cdot}023$, 0·034) which is a **3d**–3*d* system. When to the nickel matrix impurities from the 3*d* series are added, it was seen earlier that there is a peaking in the residual resistivity and a change of sign of the thermoelectric power when the 3*d* impurity is chromium. Such a system would be very interesting to probe with polarised neutrons. The measured magnetic structure amplitudes in $Ni_{1-c}Cr_c$ ($c = 0{\cdot}023$, 0·034) together with those of Ito and Akimitsu for $c = 0{\cdot}045$ were fully analysed in Fourier space using the projection operator formalism to obtain the site moment and the asphericity parameter. A multiband CPA calculation using realistic density of states carried out by us explained quite well the observed evolution of the site moment and asphericity parameter with increasing Cr concentration, and also predicted correctly the Cr concentration at which this alloy becomes paramagnetic.

6. Spin wave dispersions and exchange interactions

I have so far discussed the information provided by neutrons concerning the static or structural properties of magnetic materials, including moment density distributions.

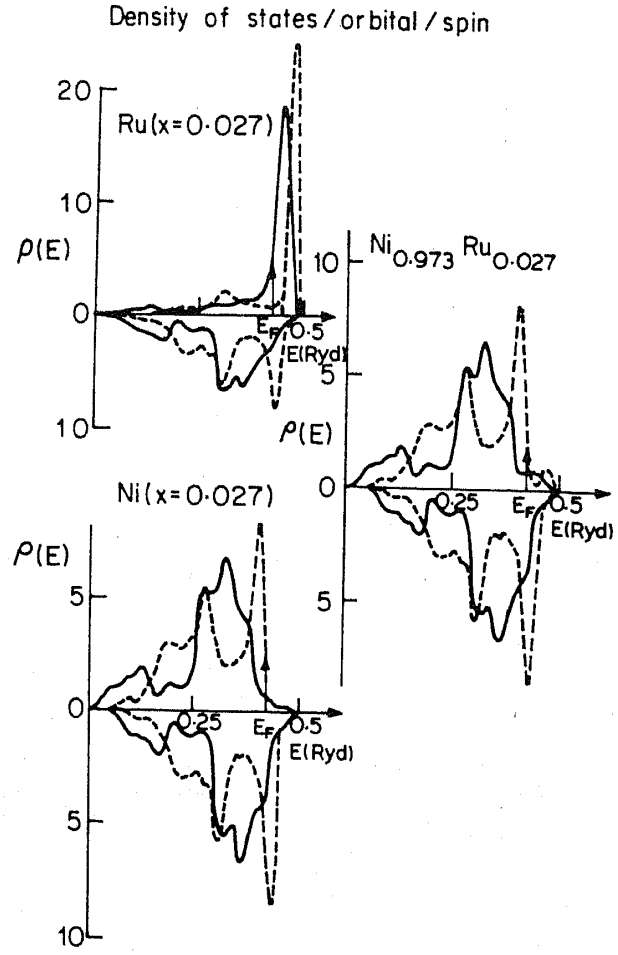

Figure 11. Density of states of the $Ni_{1-x}Ru_x$ and their constituents obtained from multiband CPA. The curves above and below the energy axis correspond to spin-up and spin-down states respectively. Continuous and broken curves are e_g and t_{2g} states respectively.

Neutrons are equally informative with respect to the energies of interactions in magnetic solid. The most detailed information of the nature and strength of the exchange coupling existing between pairs of magnetic atoms can be obtained by mapping the dispersion of spin waves in the medium. Spin wave energies increase rather rapidly with their wave-vector and therefore special techniques and high neutron fluxes are necessary for measurements involving explicit neutron energy analysis. However, using polarised neutrons and measuring the diffuse scattering from a magnetic crystal which is mis-set from its Bragg position, it is possible to map appreciable portions of the acoustic branch of the spin wave dispersion relation and obtain estimates of the exchange interaction and the anisotropy energy. Our measurements on $MnFe_2O_4$ are shown in figure 12. The use of polarised neutrons permits great accuracy in that one is able to eliminate the contributions to the intensity due to competing processes such as phonon and magnet-vibrational scattering. J_{AB}, the intersublattice exchange interaction in $MnFe_2O_4$ from these measurements is 19 K which is substantially smaller than in Fe_3O_4 ($J_{AB} = 28$ K) and agrees with the fact that $MnFe_2O_4$ has a lower Curie temperature. It also establishes that Fe^{3+} (A)-Fe^{3+} (B) interaction is very strong in the

spinel structure. The higher temperature results of figure 12 show a rapid softening of the spin waves (magnons) as the Neel point (570 K) of $MnFe_2O_4$ is approached.

A knowledge of the dominant exchange integral (such as J_{AB}) in spinels and other magnetic insulators is of great importance in understanding their phenomenology and systematics. As mentioned earlier, mapping out spin wave dispersion relations using explicit energy analysis of the scattered neutron demands much higher neutron fluxes and is quite time-consuming. Furthermore, single crystal specimens of fairly large dimension are required. An alternative method which was extensively exploited at Trombay was to study the energy distribution of neutrons (conventionally of low energy) scattered by the polycrystalline material in its paramagnetic state. When there is no residual order among spins and at large scattering angles, it has been shown by de Gennes that the second moment of the energy transfer suffered by the neutron is directly related to the exchange integral

$$\langle h^2\omega^2 \rangle = 8\pi/3\, S(S+1)\Sigma Z_i J_i^2,$$

where J_i is the exchange integral with Z_i being the number of magnetic neighbours in the ith shell. Clearly this powerful technique is most appropriate when only one exchange interaction is dominant. Figure 13 displays a typical energy distribution obtained in the case of $TlMnF_3$ which lead to a nearest neighbour exchange interaction of 3 K. We have also shown that $TlMnF_3$ assumes an antiferromagnetic ordering near

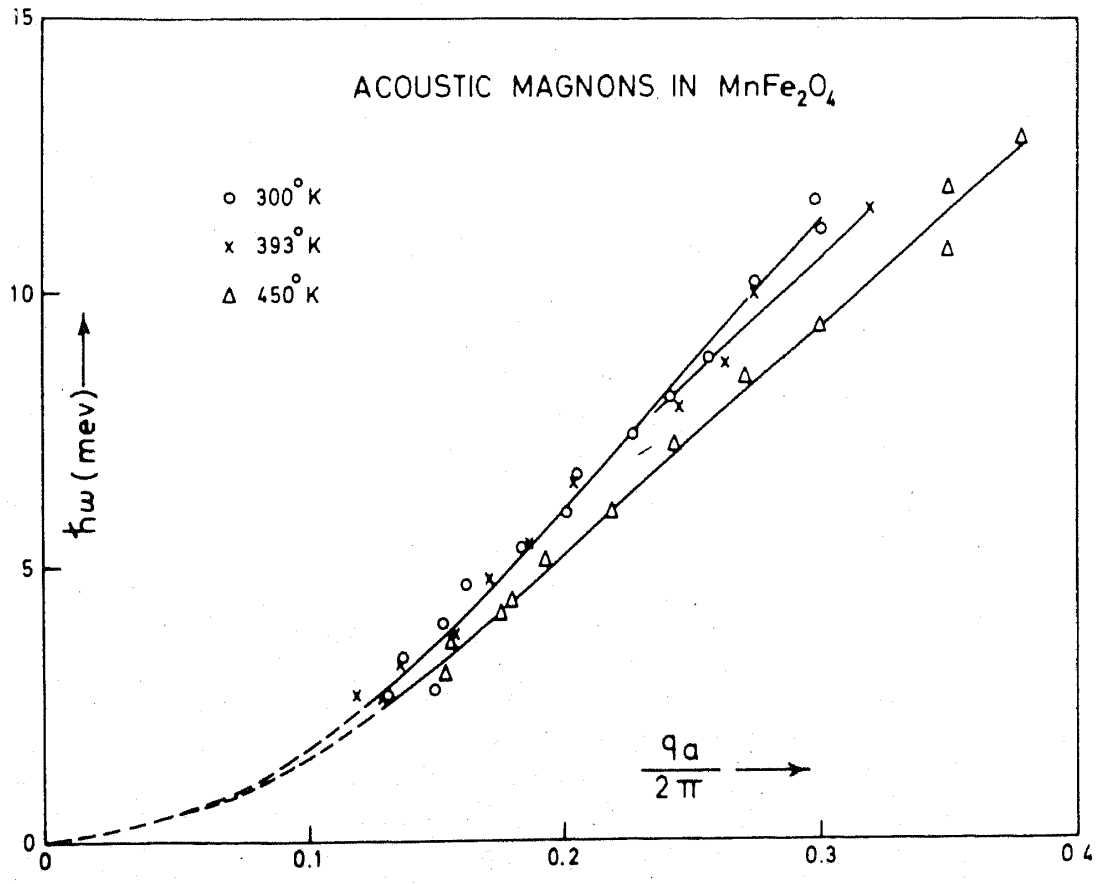

Figure 12. Acoustic spin-wave dispersion curves in $MnFe_2O_4$, at three temperatures. Note the 'softening' of the spin waves as T_N is approached.

4 K. Exchange integrals measured for some compounds by this method are summarised in table 2 together with those derived from spin wave dispersions.

The absence of magnetic short range order in the above analysis should be emphasised. Any residual ordering present will vitiate these results as demonstrated in the case of MnO where pronounced residual ordering exists at temperatures well above the Neel point of 122 K.

Time-of-flight spectra taken on MnO above T_N indicated the possible existence of spin-wave-like excitations. Madhav Rao has, however, point out that scattering from such materials cannot be interpreted in terms of spin-wave like excitations. The magnetic short-range order resembles closely the spatial short range order in liquids.

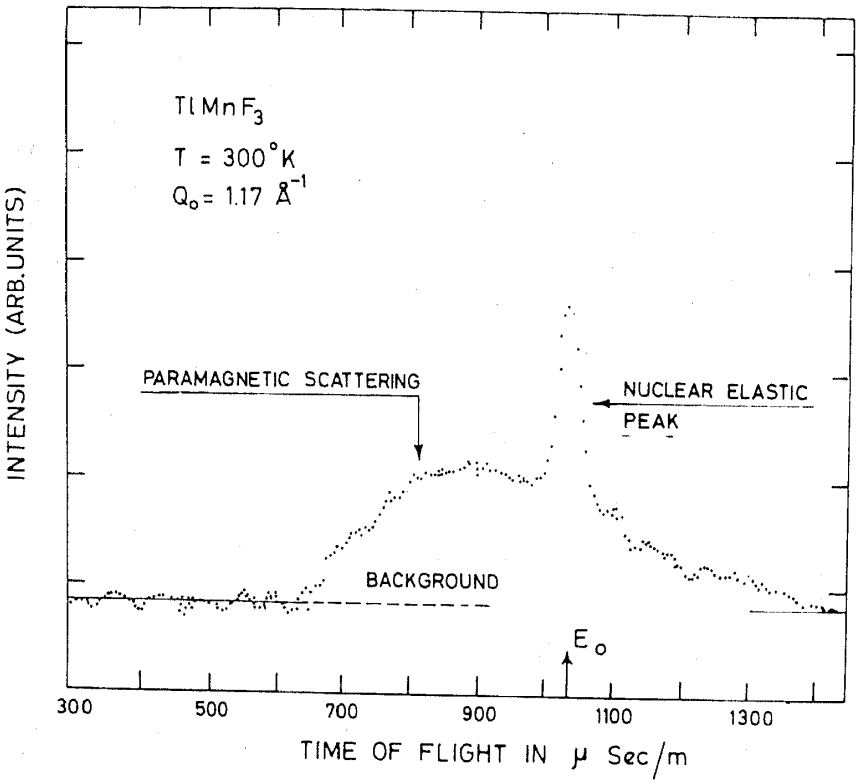

Figure 13. The neutron time-of-flight spectrum scattered from $TlMnF_3$ powder at room temperature at scattering angle 45°.

Table 2. Exchange integrals (in K) measured by paramagnetic neutron scattering and for spin wave dispersion fits

Substance	From spin wave dispersion J_1, J_2, J_3	From paramagnetic scattering J_1, J_2, J_3
MnF_2	0·08, −1·76, 0·05	$J_1 J_2 J_3 = -1·79$
$KMnF_3$	−3·8, −0·11	−3·12, −
$RbMnF_3$	−3·4, 0·0, 0·0	−3, 3, −, −
FeF_2	0·70, −2·65, −0·3	−, −3·0, −

Using the analogy of scattering by a liquid he has shown that the apparent energy shifts in such spectra can be explained without recourse to any inelastic scattering due to collective excitations.

7. Form factors from polarised neutron studies on polycrystalline magnetic compounds

In §4, I had mentioned that polarised neutrons are powerful probes to resolve ambiguities in the magnetic structure determination of polycrystalline magnetic materials. Recently we applied this technique to an interesting class of transition metal nitrides, namely Fe_4N and Mn_4N. These are cubic systems with the nitrogen atom occupying the body centre of a face-centred cube of transition metal atoms. The most interesting feature of these compounds is the fact that because of the presence of the interstitial nitrogen atom, the corner and face centre transition metal atoms have different environments and exhibit different magnetic moments.

The polarised neutron diffraction patterns were interpreted by us to obtain distinct magnetic form factors for the cube corner and face centre transition metal ion. In the case of Fe_4N, the form factor of the face-centre iron atom is broader than that of the cube corner iron atom, indicating that the unpaired electron distribution in the former is more compressed than that of the latter. Interestingly, just the opposite features were seen in Mn_4N, with the face-centre manganese atom having an unpaired electron distribution more spread out than that of the cube-corner atom.

This is the first time that polarised neutron powder data have been used to identify two distinct form factors in a unit cell. Another interesting feature which was observed in Mn_4N is that the first two of its reflections, the (100) and (110) present themselves as the two good candidates for providing polarised neutrons. An evaluation of their magnetic structure factors leads to the prediction of a polarised efficiency of 99·6 % and 94·8 % for the (100) and (110) planes respectively. Furthermore, the polarisation state of the neutron for these two planes is in opposite directions. This then offers the fascinating possibility of producing polarised monochromatic neutrons of either state of polarisation by rotating the crystal from one reflection to the other, without the use of electronic flipping devices. However, good single crystals of Mn_4N required for this purpose have not been grown so far. In these investigations, we had the collaboration of my student Marsongkohadi and others of the Bandung Institute of Technology, Indonesia.

8. Future facilities

In this brief talk I have attempted to convey to you some of the excitement in the area of neutron beam research in magnetism which my colleagues and I have shared over the last two decades or so. In the new reactor DHRUVA at Trombay, we have a neutron source more powerful than CIRUS by a factor of 2 or 3. With the installation of a cold source and a hot source (which shift substantially the reactor neutron spectrum towards lower or higher energies respectively) and the neutron guide tubes, we will have tailored neutron beams which will enable us to do a new class of experimental studies hitherto not possible at the CIRUS.

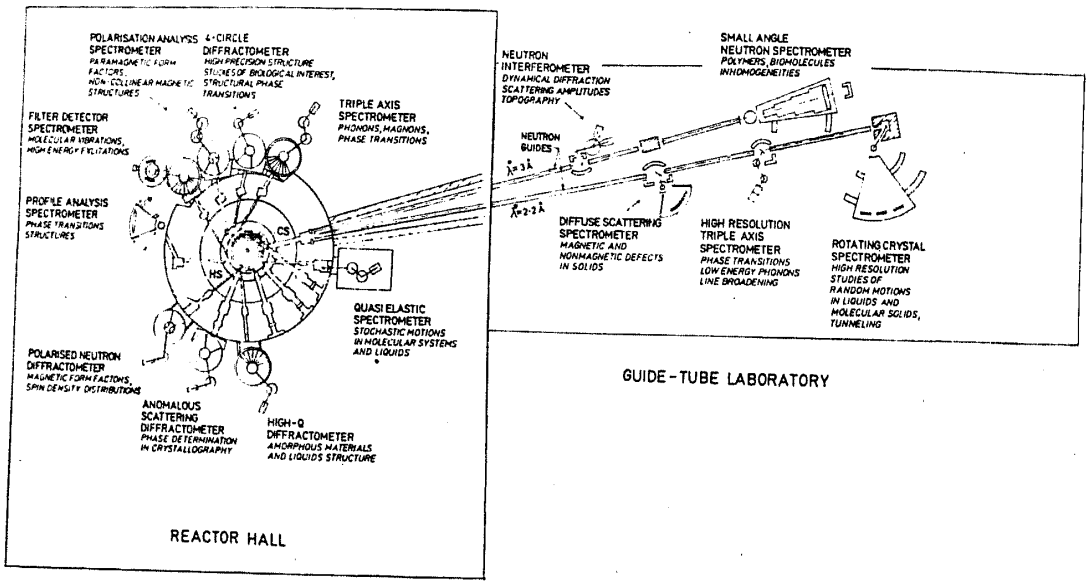

Figure 14. A full schematic layout of the neutron beam research instrumentation at the DHRUVA reactor.

With these additional features, we expect to get counting rates up by an order of magnitude in several experiments at DHRUVA. Figure 14 shows the layout of the experimental facilities which are coming up around the DHRUVA reactor. Specifically, in the area of magnetism we will have three additional facilities, namely the polarisation analysis spectrometer, the polarised neutron diffuse scattering spectrometer and the small angle spectrometer which will enable us to study paramagnetic form factors and exotic magnetic structures with great precision, probe perturbations around magnetic defects in solids and sample magnetic inhomogeneities over a range of 10 to 1000 Å. In all these developmental activities it has been our constant endeavour to design and fabricate ourselves the instrumentation composing the spectrometers, the cold and hot source facilities, the neutron guide tubes and the control and data acquisition systems. In the future we also have the possibility of much more intense neutron sources, based on accelerators at the new centre for advanced technology at Indore.

I thank you for your attention.

Bibliography

Begum R J, Madhav Rao L and Satya Murthy N S 1970 *Nucl. Phys. Solid State Phys. (India)* **130** 693
Chakravarthy R and Madhav Rao L 1981 *J. Phys.* **F11** 2071
Chakravarthy R and Madhav Rao L 1984 *Pramana (J. Phys.)* **22** 549
Chakravarthy R and Madhav Rao L 1984 *J. Magn. & Magn. Mater.* **43** 177
Chakravarthy R, Madhav Rao L and Satya Murthy N S 1980 *Pramana (J. Phys.)* **15** 207
Madhav Rao L 1972 *Phys. Status Solidi* **B50** 737
Madhav Rao L, Chakravarthy R, Jirak Z and Satya Murthy N S 1978 *Phys. Rev.* **B18** 6275
Madhav Rao L, Dasannacharya B A, Satya Murthy N S and Iyengar P K 1968 *Solid State Commun.* 7 123
Madhav Rao L, Natera M G, Satya Murthy N S, Dasannacharya B A and Iyengar P K 1968 *Solid State Commun.* **6** 593
Madhav Rao L and Satya Murthy N S 1971 *J. Phys. (Paris)* **32** Cl-617
Madhav Rao L, Satya Murthy N S, Venkataraman G and Iyengar P K 1968 *Phys. Lett.* **A26** 108

Natera M G, Murthy M R L N, Begum R J and Satya Murthy N S 1970 *Phys. Status Solidi* **A3** 959
Paranjpe S K and Begum R J 1980 *J. Magn. & Magn. Mater.* **15–18** 477
Paranjpe S K, Tendulkar S R, Madhav Rao L and Satya Murthy N S 1974 *Pramana (J. Phys.)* **3** 355
Radhakrishnan N K, Paranjpe S K, Murthy M R L N, Begum R J, Madhav Rao L and Satya Murthy N S 1972 *Nucl. Phys. Solid State Phys. India* **C14** 645
Rakhecha V C and Satya Murthy N S 1978 *J. Phys.* **C11** 4389
Rakhecha V C, Chakravarthy R and Satya Murthy N S 1978 *Pramana (J. Phys.)* **11** 159
Rakhecha V C, Madhav Rao L and Satya Murthy N S 1974 *Proc. Int. Conf. Magnetism, Moscow* **6** 262
Rakhecha V C, Rao K R and Satya Murthy N S 1976 *Proc. Conf. on Neutron Scattering, Gatlinburg, USA*, Vol. 2, p. 778
Satya Murthy N S, Begum R J, Somanathan C S, Srinivasan B S and Murthy M R L N 1969 *J. Phys. Chem. Solids* **30** 939
Satya Murthy N S and Madhav Rao L 1968 *Nucl. Phys. Solid State Phys. (India)* **A11** 177
Satya Murthy N S, Madhav Rao L, Begum R J, Natera M G and Youssef S I 1971 *J. Phys. (Paris)* **32** C1-318
Satya Murthy N S, Madhav Rao L, Natera M G and Youssef S I 1971 *Proc. Int. Conf. on Ferrites, Kyoto, Japan* (eds) Hoshin *et al* (Tokyo: University Press) p. 64
Satya Murthy N S, Natera M G, Youssef S I, Begum R J and Srivastava C M 1969 *Phys. Rev.* **181** 969
Satya Murthy N S, Somanathan C S, Begum R J, Srinivasan B S and Murthy M R L N 1969 *Indian J. Pure Appl. Phys.* 7 546
Satya Murthy N S, Venkataraman G, Usha Deniz K, Dasannacharya B A and Iyengar P K 1965 *Inelastic scattering of neutrons* (Vienna: IAEA) p. 431
Srinivasan R, Rakhecha V C, Paranjpe S K, Begum R J, Madhav Rao L and Satya Murthy N S 1974 *Proc. Int. Conf. Magnetism, Moscow* Vol. 4, p. 246
Youssef S I, Natera M G, Begum R J, Srinivsan B S and Satya Murthy N S 1969 *J. Phys. Chem. Solids* **30** 1941